AN IMPROVED DESIGN OF HI-LO MICROSTRIP LOW-PASS FILTER USING UNIPLANAR DOUBLE SPIRAL RESONANT CELLS

K. Lu, G.-M. Wang, Y.-W. Wang, and X. Yin

Missile Institute
Air Force Engineering University
Sanyuan 713800, China

Abstract—A novel microstrip resonator, uniplanar double spiral resonant cell (UDSRC) is analytically investigated to access the controllability of its bandstop property and one hi-lo microstrip lowpass filter using UDSRCs with enhanced frequency selectivity and rejection level is also presented. The equivalent circuit corresponding to each part of UDSRC is initially proposed to describe its special bandstop property with two transmission zeros. Furthermore, analytical theories of each circuit element are introduced and the comparison of the calculated results and the fullwave-simulated ones is done to verify the proposed equivalent circuit and the analytical theories. Both the analytical investigation and parametric analysis indicate that the two transmission zeros can be controlled through tuning the primary geometrical parameters. Thus, the given property is utilized by embedding two different UDSRCs in the feed lines of the reference filter. Both the simulated and measured results indicate that the frequency selectivity and rejection level are improved effectively. The frequency selectivity of the fabricated prototype is about 65.8 dB/GHz while the stopband rejection level is more than 10 dB from 2.08 GHz to 6.62 GHz. Compared with the reference filter, the performance is improved greatly while the transversal dimension of the feed line is not increased because UDSRCs are completely embedded in the feed lines.

1. INTRODUCTION

Microstrip lowpass filters are widely utilized to suppress harmonics and spurious signals due to low weight and easy fabrication. Therefore, the microstrip lowpass filters having sharp rejection and high rejection level are of increasing demand in many RF and microwave communication systems. The conventional hi-lo microstrip lowpass filter composed of sections with different impedances has the disadvantages of flat transition from passband to stopband and relatively poor rejection level [1]. The defected ground structures (DGSs) have been introduced to broaden the stopband and sharpen the frequency selectivity effectively [2, 3]. Whereas, there is a back radiation problem which is common for DGS and additional metallic plane must be appropriately put underneath the ground of microstrip components. In [4], the low-impendence sections were constructed as fractal geometry in order to improve the performance of the passband. But, the stopband properties approximately remained unchanged and thus the given structure suffers from the poor frequency selectivity.

In our work, a novel microstrip resonator, UDSRC is utilized firstly to improve the performance of hi-lo microstrip lowpass filter. UDSRC is initially proposed in [5] and it is demonstrated that it exhibits left-handed properties for surface wave propagation due to the exotic electric and magnetic coupling properties [6, 7]. In recent years, the cross coupling phenomenon are introduced to improve the microwave components based on the left-handed transmission line [8–10]. In this letter, the fact that UDSRC embedded in the microstrip line exhibits high rejection stopband including two controllable transmission zeros is demonstrated through numerical simulation. Moreover, the equivalent circuit and the analytical theories of each circuit element are proposed. Comparison of the calculated results and the fullwave-simulated ones is implemented to verify the proposed equivalent circuit and the given analytical theories. These methods provide an effective guidance for the design of UDSRCs. Thus, this special property is utilized by embedding two UDSRCs in the feed lines. Compared with the reference filter, both the simulated and measured results indicate that the frequency selectivity and rejection level are enhanced effectively. In addition, UDSRC is completely embedded in feed line so that UDSRC can yield compact dimensions of the proposed prototype. Simultaneously, there is no back radiation problem for the proposed filter thanks to its uniplanar property.
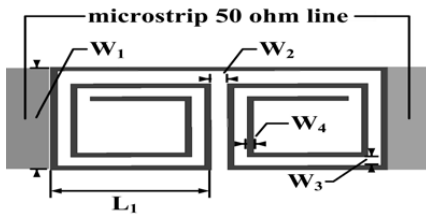
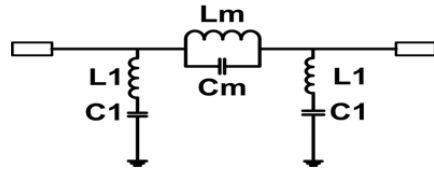**Figure 1.** Layout of the double spiral resonant cell embedded in microstrip line.

Figure 2. Proposed lossless equivalent circuit for UDSRC embedded in microstrip line.

2. EQUIVALENT CIRCUIT AND ANALYTICAL ANALYSIS OF UDSRC

The layout of UDSRC embedded in the microstrip line is presented in Fig. 1. For simplicity, $W_1 = 4.6$ mm (equal to the width of microstrip 50 ohm line), $W_3 = 0.4$ mm and $W_4 = 0.2$ mm are kept constant throughout this work. L_1 and W_2 are the primary adjustment geometrical parameters. The substrate with relative dielectric constant of 2.2 and thickness of 1.5 mm is utilized in both simulation and fabrication. The fact that UDSRC embedded in the microstrip line exhibits the stopband including two transmission zeros is demonstrated through numerical simulation. To interpret the operating principle of UDSRC embedded in the microstrip line, one equivalent circuit corresponding to each part of UDSRC is proposed in Fig. 2.

The proposed equivalent circuit is composed of two shunt-connected series LC resonator and one series-connected shunt LC resonator. Moreover, L_1 is the inductance of single rectangular spiral and C_1 is the capacitance between the conducting strips forming the single spiral and the ground plane; L_m denotes the inductance of conducting strip with the length of $2L_1 + W_2$, which connects the two spirals and C_m is the capacitance between the adjacent strips of the two spirals referenced in [11]. Based on the above equivalent circuit, f_{sh}, the resonant frequency of the series LC resonator and fse, the resonant frequency of the shunt LC resonator are expressed in Equations (1) and (2), respectively.

$$f_{sh} = \frac{1}{M(2\pi\sqrt{L_1 \cdot C_1})} \tag{1}$$

$$f_{se} = \frac{1}{M(2\pi\sqrt{L_m \cdot C_m})} \tag{2}$$

where M is a modified factor required in practical calculation, because the circuit parameters are all evaluated with limited precision.

Furthermore, when the given equivalent circuit is utilized as a directive design tool for UDSRC, the analytical theories of each circuit element are necessary. Firstly, L_1 is given by Equation (3) referenced in [12].

$$L_1 = \frac{\mu_0}{2\pi} l_{ASR} \left[\ln \left(\frac{l_{ASR}}{2W_4} \right) + \frac{1}{2} \right]$$

$$l_{ASR} = 4l - [2(N+1) - 3/N](W_3 + W_4) \tag{3}$$

where N is the number of the turns and l is the side length of the external turn. It is should be noted that this equation is initially utilized to describe the square spiral. Thus, for the rectangular spiral proposed in our work, $l = (L_1 + W_1)/2$ is implemented in approximation. Secondly, C_1 is approximately estimated by Equation (4) referenced in [13]

$$C_1 = \frac{1}{2} l_t W_4 \frac{\varepsilon}{h} \tag{4}$$

where l_t denotes the total length of the conducting strips forming the single spiral and h is the height of the dielectric layer. In addition, L_m is calculated with the approximate design Equation (5) referenced in [14]

$$L_m(\text{nh})$$
$$= 2 \times 10^{-4} (2L_1 + W_2) \left[\ln \left(\frac{2L_1 + W_2}{W_4 + t} \right) + 1.193 + 0.2235 \frac{W_4 + t}{2L_1 + W_2} \right] K_g \tag{5}$$

For this equation, there is a special limitation that the unit of all physical length parameters is um. t denotes the thickness of the conducting strip which is set to be 18 μm. For simplicity, the correction factor, Kg is chosen to be 1 in the calculation. Subsequently, the value of Cm is roughly predicted using Equation (6) which describes the capacitance between two parallel strips referenced in [15]

$$C_m \approx \frac{2(W_1 - W_3 - W_4)}{\pi} \varepsilon \arccos \left(\frac{2W_4}{W_2} \right) \tag{6}$$

Therefore, when the geometrical parameters are given, the circuit parameters can be derived from the above equations and the frequency response of the proposed equivalent circuit is then determined. Based on above analysis, the calculated resonant frequencies roughly correspond to the two transmission zeros in fullwave simulation. In order to verify the proposed equivalent circuit and the analytical theories, three UDSRCs with different dimensions are present and the results derived from the proposed equivalent circuit and analytical theories are compared with the fullwave simulated ones as shown in

Table 1. Summary of calculated circuit parameters and comparison of calculated resonant frequencies and transmission zeros derived from fullwave simulation.

	L1 nh	C1 pf	Lm nh	Cm pf	fsh GHz	fse GHz	fl GHz	fh GHz
	shunt branch		series branch		theoretical calculation		full wave simulation	
1	12.37	0.0037	9.329	0.0041	2.2001	2.3989	2.20	2.42
2	11.56	0.0034	8.383	0.0041	2.3598	2.5307	2.34	2.64
3	8.199	0.0031	6.877	0.0047	2.9363	2.6116	2.80	3.08

Note: case 1, L1=4.4mm, W2=0.6mm; case 2, L1=4.0mm, W2=0.6mm; case 3, L1=3.3mm, W2=0.7mm. 'fl' denotes the transmission zero in lower frequency band. 'fh' denotes the transmission zero in higher frequency band. Blue background indicates that the frequencies are the lower ones and pink background indicates that the frequencies are the higher ones.
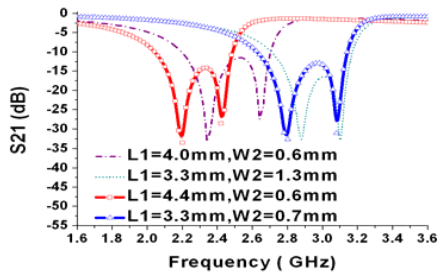

Figure 3. Variation of S_{21} for USDRC embedded in the microstrip line with the geometrical parameters 'L_1' and 'W_2'.

Table 1. Simultaneously, the calculated circuit parameters are also listed in Table 1. The modified factor, M is set to 3.36.

As shown in Table 1, reasonable agreement is achieved between the theoretically calculated frequencies and the fullwave simulated results. This means that the proposed equivalent circuit and the analytical theories are both valid and effective, which can accelerate the design process of UDSRC greatly. It is can be seen that, from the above equations, the circuit parameters can be controlled by tuning the primary geometrical parameters and thus the bandstop property can be adjusted directively. In order to verify this conclusion further, one parametric analysis is done. Fig. 3 depicts the variation of the transmission coefficients with the two geometrical parameters. It is seen that the center frequency, the bandwidth and even the rejection level can be controlled effectively through tuning L_1 and W_2.

3. DESIGN OF THE PROPOSED FILTER USING UDSRCs

Based on the above conclusions, the method of integrating UDSRC with the hi-lo microstrip lowpass filter is expected to enhance the frequency selectivity and rejection level. In this paper, this idea is realized by embedding UDSRCs in the feed lines of the reference filter as shown in Fig. 4. The given structure avoids changing the geometry of the reference filter and thus the property of UDSRC can be tuned independently to get the satisfactory performance, which yields more flexibility on the filter design. The reference filter is constructed by cascading one high impedance section and two low impedance sections with alternative lengths while the detailed layout is determined according to the standard procedure in [4]. The characteristic impedances of the high and the low impendence sections are set to 116.7 ohm and 17.5 ohm, respectively, where the electrical length of each transmission line section is got through the design formulas in [4] and Ansoft Designer TRL Calculator. It should be emphasized that, in order to enhance the frequency selectivity, the transmission zero in lower frequency band should be adjusted to be in the vicinity of the passband edge of the reference filter. Simultaneously, the transmission zero in higher frequency band together with the other two transmission zeros provided by another UDSRC should fall in the stopband to improve the rejection level. The results from the proposed analytical theories will provide a good starting point for the simulation, but further minor adjustments are still necessary. Consequently, satisfactory performance is achieved and the geometrical parameters are summarized in Fig. 4.
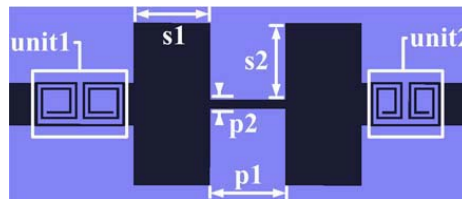

Figure 4. Layout of the proposed hi-lo microstrip lowpass filter using UDSRCs. The geometrical parameters of referenced hi-lo microstrip lowpass filter are listed as follow: $s_1 = 8$ mm, $s_2 = 8.6$ mm, $p_2 = 0.9$ mm, $p_1 = 8.1$ mm. For unit 1, L_1 and W_2 are equal to 4.4 mm and 0.6 mm, respectively. For unit 2, L_1 and W_2 are equal to 3.3 mm and 0.7 mm, respectively.

What is more important, even the longer length of the two UDSRCs, 9.2 mm, is a small fraction of the wavelength at the cutoff frequency of the reference filter (approximately $\lambda/15$) so that UDSRC can result in the compact dimensions. Moreover, UDSRCs is completely embedded in 50 ohm microstrip line which makes it compatible with microstrip components without increasing the transversal dimension.

4. SIMULATION AND EXPERIMENTAL RESULTS

The reference filter and the proposed filter using UDSRCs are fabricated and the photographs of the given prototypes are shown in Fig. 5. To provide space for the connectors, two 10 mm long 50 ohm lines have been cascaded at the input and output ports. Thus, the physical length of the proposed filter using UDSRCs is about 63 mm. The reflection and transmission coefficients were measured using an Anritsu ME7808A vector network analyzer while the simulated and measured results of these two filters are shown in Fig. 6 and Fig. 7, respectively. In these two figures, 'A' represents the reference filter while 'B' represents the proposed filter using UDSRCs. Measured results indicate that the 3-dB cutoff frequency of B filter is at 1.919 GHz and this filter has excellent frequency selectivity which is approximately 65.8 dB/GHz (S_{21} being-3 and -25.02 dB at 1.919 and 2.253 GHz, respectively). The measured stopband attenuation level is more than 10 dB from 2.08 GHz to 6.62 GHz. Moreover, the measured the 3-dB cutoff frequency of the A filter is 2.37 GHz while the stopband more than 10 dB is from 4.06 GHz to 5.88 GHz. The frequency selectivity of the reference filter is about 3.42 (S_{21} being -3 dB and
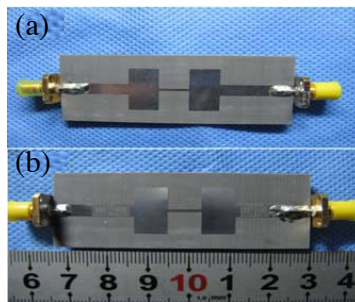

Figure 5. The photographs of the fabricated prototypes. (a) The reference hi-lo microstrip lowpass filter. (b) The proposed filter using UDSRCs.
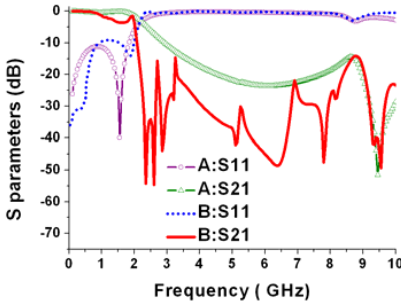
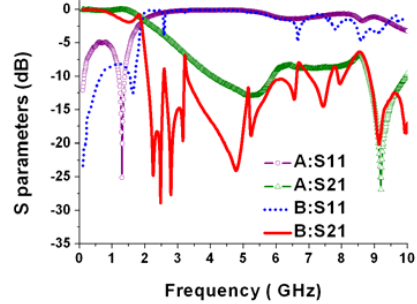**Figure 6.** The simulated S parameters of the reference filter and the proposed filter using UDSRCs.

Figure 7. The measured S parameters of the reference filter and the proposed filter using UDSRCs.

-13.4 dB at 2.37 GHz and 5.29 GHz, respectively). Based on the above results, it is seen that the frequency selectivity and rejection level are both modified effectively through introducing UDSRCs within the feed lines. Thus, the similar conclusions can be derived from the simulated results shown in Fig. 6. To sum up, there are some minor discrepancies between the simulated and measured results, possibly due to the fabrication inaccuracy, but a great agreement is presented on the whole. The given results reveal that the proposed method is very proposing for the design of performance-enhanced hi-lo microstrip lowpass filter.

5. CONCLUSION

To improve the frequency selectivity and rejection level of the conventional hi-lo microstrip filter, a novel method using UDSRCs is proposed. UDSRC embedded in the microstrip line exhibits bandstop property with two controllable transmission zeros. In order to interpret this behavior, the equivalent circuit and the analytical theories of the circuit parameters are proposed, verified and utilized as an effective design tool. Two different UDSRCs are embedded in the feed lines of the reference filter to improve the performance. Both the reference filter and the proposed filter using UDSRCs are fabricated and the simulated and measured results show that the frequency selectivity and rejection level are improved greatly. Moreover, the given method can be utilized effectively in many other applications.

REFERENCES

1. Hong, J.-S. and M. J. Lancaster, *Microstrip Filters for RF/Microwave Applications*, Wiley, New York, 2001.

2. Ahn, D., J.-S. Park, C.-S. Kim, J. Kim, Y. Qian, and T. Itoh, "A design of the low-pass filter using the novel microstrip defected ground structure," *IEEE Trans. Microw. Theory Tech.*, Vol. 49, No. 1, 86–93, Jan. 2001.

3. Abdel-Rahman, A. B., A. K. Verma, A. Boutejdar, and A. S. Omar, "Control of bandstop response of Hi-Lo microstrip low-pass filter using slot in ground plane," *IEEE Trans. Microw. Theory Tech.*, Vol. 52, No. 3, 1008–1013, Mar. 2004.

4. Chen, W.-L., G.-M. Wang, and Y.-N. Qi, "Fractal-shaped Hi-Lo microstrip low-pass filters with high passband performance," *Microwave and Optical Technology Letters*, Vol. 49, No. 10, 2577–2579, Oct. 2007.

5. Guo, Y., G. Goussetis, A. P. Feresidis, and J. C. Vardaxoglou, "Efficient modeling of novel uniplanar left-handed metamaterials," *IEEE Trans. on Microw. Theory and Tech.*, Vol. 53, No. 4, 1462–1468, Apr. 2005.

6. Kokkinos, T., A. P. Feresidis, and J. C. Vardaxoglou, "On the use of spiral resonators for the design of uniplanar microstrip-based left-handed metamaterials," *Proc. European Conference on Antennas and Propagation*, Nice, France, 2006.

7. Kokkinos, T., A. P. Feresidis, and J. C. Vardaxoglou, "Equivalent circuit of double spiral resonators supporting backward waves," *Loughborough Antennas and Propagation Conference*, 289–292, Loughborough University of Technology, UK, 2007.

8. Keshavarz, R., M. Movahhedi, A. Hakimi, and A. Abdipour, "A novel broad bandwidth and compact backward coupler with high coupling level," *Journal of Electromagnetic Waves and Applications*, Vol. 25, No. 2–3, 283–293, 2011.

9. Huang, J.-Q. and Q.-X. Chu, "Compact UWB band-pass filter utilizing modified composite right/left-handed structure with cross coupling," *Progress In Electromagnetics Research*, Vol. 107, 179–186, 2010.

10. Abdelaziz, A. F., T. M. Abuelfadl, and O. L. Elsayed, "Realization of composite right/left-handed transmission line using coupled lines," *Progress In Electromagnetics Research*, Vol. 92, 299–315, 2009.

11. Kokkinos, T. and A. P. Feresidis, "Low-profile folded monopoles with embedded planar metamaterial phase-shifting lines," *IEEE*

Trans. Antennas Propagat., Vol. 57, No. 10, 2997–3008, Oct. 2009.

12. Bilotti, F., A. Toscano, and L. Vegni, "Design of spiral and multiple split-ring resonators for the realization of miniaturized metamaterial samples," *IEEE Trans. Antennas Propagat.*, Vol. 55, No. 8, 2258–2267, Aug. 2007.

13. Yue, C. P. and S. S. Wang, "A physical model for planar spiral inductors on silicon," *International Electron. Devices Meeting Technical Digest*, 155–158, Dec. 1996.

14. Chi, C.-Y. and G. M. Rebeiz, "Planar microwave and millimeter-wave lumped elements and coupled-line filters using micro-machining techniques," *IEEE Trans. Microw. Theory Tech.*, Vol. 43, 730–738, Apr. 1995.

15. Wang, J., S. Qu, Z. Xu, H. Ma, Y. Yang, and C. Gu, "A controllable magnetic metamaterial: Split-ring resonator with rotated inner ring," *IEEE Trans. Antennas Propagat.*, Vol. 56, No. 7, 2018–2022, Jul. 2008.